PARAMETER OPTIMIZATION FOR THE LOW FREQUENCY LINACS IN THE NLC *

Z. Li†, T.O. Raubenheimer, K. Bane, J.C. Sheppard, R.H. Miller
Stanford Linear Accelerator Center, Stanford University, Stanford, CA 94309

Abstract

In the present Next Linear Collider (NLC) design, S and L-band linacs are used to accelerate the beams to 10 GeV, where they are injected into the main X-band linacs. As injectors for the main accelerator, these linacs are required to deliver clean beams while being reliable and cost effective. These requirements set stringent tolerances on the design of the accelerators. There are two types of misalignment tolerances that are of great concern: cell-to-cell and structure-to-structure tolerances, which are dominated by long- and short-range wakefield effects, respectively. For a given lattice design, the structure-to-structure tolerance (which has strong impacts on girder configurations) is mainly determined by the global parameters such as the average iris size, the length and the type of the structure. This paper will discuss the optimization of the structure parameters to allow looser structure-to-structure tolerances; the cell-to-cell tolerance is related to the details of the single structure design and will not be addressed here. The optimization described here was based on a cost model for NLC and a wakefield scaling law for the tolerance estimations.

1 INTRODUCTION

The Next Linear Collider (NLC) is a $e^+ - e^-$ linear collider that will be used to probe the physics phenomena at a center of mass around 1 TeV [1, 2]. The main linacs of this collider are based on X-band rf (11.424 GHz) technology. In the injector which accelerates the e^+ and e^- beams to 10 GeV, the beams are accelerated in lower frequency linacs operating at the L-band (1.428 GHz) and S-band (2.856 GHz). There are a total of ten low frequency linacs in the injector system which are listed in Table 1; a detailed discussion of the NLC injector systems is presented in Ref. [3].

Table 1: NLC low frequency linacs

Linacs	rf	N	E (GeV)	Q($\times 10^{10}e$)	I (A)
e^+ capture	L	1	0.25	7.8	4.5
e^+ booster	L	1	1.75	1.6	0.91
e^+ drive	S	1	6	1.45	0.83
e^- booster	S	1	1.9	1.45	0.83
pre-linacs	S	2	8	1.15	0.66
EC	L	2	0.1	1.45	0.83
BC1	L	2	0.1	1.45	0.83

* Work supported by the DOE, contract DE-AC03-76SF00515.
† email: lizh@slac.stanford.edu

Because of differences in the beam parameters in these linacs, the issues concerning the accelerator design are also quite different. In the L-band e^+ capture and booster linacs, the beam has a large emittance and energy spread and the primary issue is the aperture. A larger aperture in the structure allows larger beta functions, easing the strength and the tolerance requirements on the quadrupole magnets.

In the S-band pre-linacs, the beam emittance is small and the bunch length is short. The primary issues here are the emittance degradation and multi-bunch BBU associated with the long- and short-range wakefields in the structure. The tight emittance dilution and BBU requirements set stringent limits on the structure tolerances. The short-range wakefields, which are related to the average parameters of a structure, dominate the structure-to-structure tolerances, while the long-range wakefields, which are related to the details of the structure design, control the cell-to-cell tolerance of a structure. This paper will focus on the structure-to-structure tolerance associated with the short-range wakefields.

The beam loading voltage in these linacs will be compensated by using the ΔT scheme [4], except in the e^+ capture where the beam current is extremely high and the ΔF scheme is used. With the ΔT scheme, the structure design is tightly coupled to the beam loading conditions. Both the L- and S-band linacs will have a single structure design for all the corresponding linacs. We have optimized the L-band structure for the e^+ booster parameters while the S-band structure was optimized for the pre-linac parameters.

2 S-BAND LINACS

Both the structure tolerance requirements and the cost of the S-band linacs are dominated by the pre-linacs and thus the structure optimization is based on the pre-linac parameters. The cost and tolerance models we used are similar to the ones used for the ZDR [1] cost and tolerance calculations.

2.1 Cost estimation

A simple cost model, Eq. (1), is used to estimate the cost of the pre-linacs.

$$\begin{aligned} Cost = \quad & N_s(S_s + S_{bpm}) \\ + \quad & N_s M_s(Q_q + Q_{ps} + Q_{bpm}) \\ + \quad & N_M N_k(K_k + k_{rf}) \\ + \quad & N_M(P_{SLED} + P_{wg} + P_{phase} + P_{modul}) \end{aligned} \tag{1}$$

$$+ \quad \frac{N_s L}{S_f}(F_{tunnel} + F_{alcove})$$
$$+ \quad \frac{N_s L}{S_f}(V_{pipe} + V_{rf})$$

where the cost of the parts are

S_s, S_{bpm}	structure, structure BPM
Q_q, Q_{ps}, Q_{bpm}	quad, quad power supply, quad BPM
K_k, K_{rf}	klystron, klystron rf drive
$P_{SLED}, P_{wg},$	SLED-I system, waveguide,
P_{phase}, P_{modul}	phase control, modulator
F_{tunnel}, F_{alcove}	tunnel and alcove
V_{pipe}, V_{rf}	vacuum pipe and rf

N_s, N_M are the total number of structures and modules respectively. A 10% overhead is assumed in the number of modules for the linacs. N_k is the number of klystrons per module ($N_k = 2$ for ΔT compensation scheme) and M_s is the number of quads per structure; the focusing in the pre-linacs is provided with the FODO lattices. Finally, S_f is the filling factor of the accelerator structures in the linac which is assumed to be 80%.

In the calculation, we assumed that the structure cost is dominated by the assembly and coupler costs and thus the cost of the linacs scales with the number of structures and not the structure length. All cost estimations were scaled to a linac design based on a 3-meter SLAC-type accelerator structure.

2.2 Structure-to-structure tolerance

The structure-to-structure tolerance is associated with the short-range wakefield effects of the structure which depends mainly on the average parameters of the structure, e.g. the average aperture and length. To the lowest order, the short-range wakefield scales as the 4th power of the average iris radius. Assuming the β functions are scaled with the structure length, the structure-to-structure tolerance is proportional to

$$y_{tol} \propto \frac{a^4}{L_{acc}} \tag{2}$$

where a is the average iris radius and L_{acc} is the total net accelerator length.

2.3 Length vs structure-structure tolerance

In a constant gradient traveling wave structure, the unloaded acceleration voltage of a accelerator section is

$$V = \sqrt{P_{in} R L (1 - e^{-2\tau})} \tag{3}$$

and the transient beam loading voltage ($0 < t < t_f$) is

$$V_{beam} = -\frac{R I_0 L}{2(1 - e^{-2\tau})}\left(1 - e^{-\frac{\omega t}{Q}} - \frac{\omega e^{-2\tau}}{Q} t\right) \tag{4}$$

where L is the structure length, R is the shunt impedance per unit length, t_f is the filling time, and $\tau = \omega t_f / 2Q$ is the attenuation constant. With the same τ (or t_f) factor, the acceleration and beam loading voltages are proportional to $\sqrt{RL}$ and RL (or $\sqrt{Rv_g}$ and Rg_v, $v_g = L/t_f$) respectively. Since v_g has a stronger dependence on the iris radius than R, the rf efficiency is higher in a longer structure.

The group velocity of a traveling wave structure scales approximately as a^3. The structure-to-structure tolerance then scales as

$$y_{tol} \propto \left(\frac{L}{t_f}\right)^{4/3} / L_{acc} = \frac{L^{1/3}}{t_f^{4/3}}\left(\frac{L}{L_{acc}}\right) \tag{5}$$

where L/L_{acc} represents the rf efficiency of the linac. It is clear that the gain in tolerance with a longer structure length comes from the gain in rf efficiency, filling time change due to change in beam loading, and the lengthening of the structure.

The 3- and 4-meter SLAC-type structures (DLWG) were simulated to study the cost and tolerance dependences on the structure length. Results for the two cases are shown in the first two rows in Table 3. It is clear that a longer structure is beneficial for both the rf efficiency and the structure-to-structure tolerance. Fewer modules are needed in the 4-meter design as a result of a better rf efficiency which results in saving about 8% in rf power. The optimal filling time for the 4-meter design is 625 ns, slightly shorter than the 665 ns for the 3-meter design due to a stronger beam loading and the structure-to-structure tolerance is improved by about 30%. Additional increases in the structure length may further improve the efficiency and tolerances, however, such a long structure is thought to be significantly more difficult to manufacture.

2.4 Cell profile optimization

In the X-band main linac design, the shunt impedance was optimized to improve the rf efficiency by shaping the cell geometry. A round cell contour (RDS) was obtained as shown in Fig. 1, which gives about 15% better shunt impedance as compared to the standard DLWG. The optimized RDS cell profile can be used in the S-band design for the same purpose. Alternatively, one can use the RDS design to improve the structure tolerance by further opening the iris while maintaining the same rf efficiency. Table 2 shows a comparison between the DLWG and RDS parameters for a S-band cell.

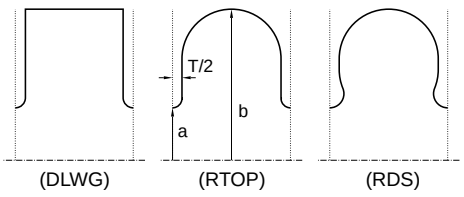

Figure 1: Traveling wave structure cell profiles: DLWG) standard; RTOP) round top; RDS) round contour.

Table 2: A comparison between DLWG and RDS cells

Type	a (mm)	R (MΩ/m)	v_g/c
DLWG	13	54.0	0.0195
RDS	14	54.0	0.0190

For the same R and v_g, the RDS cell yields a much larger iris size. Since the structure tolerance scales as the 4th power of the iris radius, the RDS design will further relax the structure-to-structure tolerance. The third row in Table 3 shows the result for a 4-meter RDS design. The tolerance is about 25% better than the 4-meter DLWG case. The rf efficiencies and costs are comparable.

Table 3: Comparison of the S-band DLWG and RDS structures. *) 4-structure/module; **) 6-structure/module.

Type	L(m)	N_{module}	Cost	a_{av}(mm)	tol
DLWG*	3.0	27	1.0	12.85	1.00
DLWG*	4.0	25	1.0	14.69	1.29
RDS*	4.0	25	1.0	15.40	1.53
RDS**	4.0	22	1.09	15.72	1.43

The results shown in the first three rows of Table 3 are for linacs with a 4-structure per module configuration. The loaded gradient in these cases is about 22 MV/m. A lower gradient design of 17 MV/m has been consider for the NLC S-band linacs. The low gradient design uses the same RDS 4-meter structures but one rf power station will power a module of six structures instead of four. The results of the low gradient design are shown in the last row of Table 3. Due to the longer linac length, the tolerance is slightly tighter and the cost is slightly higher however the overall tolerance improvement is still $> 40\%$ compared to the 3-meter DLWG design.

3 L-BAND LINACS

The beam emittance and energy spread are large in the L-band capture and booster linacs. Strong focusing lattice are required for these linacs to control the beam size. A larger aperture in the structure would allow larger beta functions, which would relax the tolerances on the focusing magnets. The structure alignment tolerances are loose in these linacs and thus the design goal for the L-band structures is simply to maximize the structure aperture.

A length of 5 meters is considered for the L-band structure. There is not a strong argument to use the RDS design in the L-band design. The studies in this paper are based on the RTOP cell profile, shown in Fig. 1, however, the results are applicable to a DLWG design, with minor modifications.

The L-band structure is optimized for the e^+ booster beam current. A booster module consists of six 5-meter structures. Table 4 shows a list of L-band structures with different cell disk thicknesses. The dipole mode detuning ΔF_1, which is determined by the long-range wakefield properties, also impacts the aperture, Because the linac will

Table 4: 5-meter L-band structure with RTOP cell profiles

T (mm)	ΔF_1 (%)	a_{min} (mm)	b_{max} (mm)	G_L (MV/m)
12	3	23.51	89.83	13.1
12	5	22.43	90.29	
15	3	24.37	90.08	12.92
15	5	23.13	90.52	
18	3	25.19	90.40	12.46
18	5	24.24	91.00	

be constructed from an integer number of modules, we actually can reduce the shunt impedance slightly to fully utilize five 6-structure modules. In this case, the loaded gradient in the e^+ booster is 12.4 MV/m to attain the required 1.75 GeV acceleration plus roughly 5% margin.

4 TOLERANCES

Finally, the tolerances for the S-band linacs are listed in Table 5. In the e^- booster and e^+ drive linacs, one-to-one trajectory correction is assumed where the trajectory is corrected to zero the Beam Position Monitors (BPMs) located at the focusing quadrupoles. In the pre-linacs, the trajectory will be corrected using beam-based alignment similar to that used in the main linac [6]. The tolerances in the L-band e^+ booster linac are slightly looser than those in the e^- booster linac.

Table 5: Tolerances for the S-band linacs (rms)

Linac	Quad	BPM to quad	Struct-struct
e^- booster e^+ drive	200 μm	200 μm	500 μm
pre-linac	15 μm	15 μm	40 μm

5 REFERENCES

[1] NLC ZDR Design Group, "Zeroth-Order Design Report for the Next Linear Collider," SLAC Report 474 (1996).

[2] NLC Accelerator Physics Web pages from http://www-project.slac.stanford.edu/lc/nlc-tech.html.

[3] J. C. Sheppard and et. al., "The NLC Injector System," this conference.

[4] Z. Li and et. al., "Beam loading compensation for the Low RF Frequency Linacs of the NLC," this conference.

[5] Z. Li and et. al., "RDDS Cell Design and Optimization for the NLC linac," this conference.

[6] P. Tenenbaum, "Simulation Studies of Main Linac Steering in the Next Linear Collider," this conference.